SPRY2 loss enhances ErbB trafficking and PI3K/AKT signalling to drive human and mouse prostate carcinogenesis

*Meiling Gao[1], Rachana Patel[1], Imran Ahmad[1,2], Janis Fleming[1], Joanne Edwards[2], Stuart McCracken[3], Kanagasabai Sahadevan[3], Morag Seywright[4], Jim Norman[1], Owen Sansom[1], Hing Y. Leung[1,2]**

Keywords: AKT; ErbB receptor; prostate cancer; PTEN; Sprouty 2

DOI 10.1002/emmm.201100944

Received September 10, 2011
Revised April 06, 2012
Accepted April 20, 2012

Loss of SPRY2 and activation of receptor tyrosine kinases are common events in prostate cancer (PC). However, the molecular basis of their interaction and clinical impact remains to be fully examined. SPRY2 loss may functionally synergize with aberrant cellular signalling to drive PC and to promote treatment-resistant disease. Here, we report evidence for a positive feedback regulation of the ErbB-PI3K/AKT cascade by SPRY2 loss in *in vitro* as well as pre-clinical *in vivo* models and clinical PC. Reduction in SPRY2 expression resulted in hyperactivation of PI3K/AKT signalling to drive proliferation and invasion by enhanced internalization of EGFR/HER2 and their sustained signalling at the early endosome in a PTEN-dependent manner. This involved p38 MAPK activation by PI3K to facilitate clathrin-mediated ErbB receptor endocytosis. Finally, *in vitro* and *in vivo* inhibition of PI3K suppressed proliferation and invasion, supporting PI3K/AKT as a target for therapy particularly in patients with PTEN-haploinsufficient-, low SPRY2- and ErbB-expressing tumours. In conclusion, SPRY2 is an important tumour suppressor in PC since its loss drives the PI3K/AKT pathway via functional interaction with the ErbB system.

INTRODUCTION

Prostate cancer (PC) is the most common cancer among aging men worldwide. Both prostate organogenesis and tumourigenesis are critically dependent on androgen receptor (AR) signalling (Potente et al, 2007). Treatment for patients with locally advanced or metastatic PC remains unsatisfactory and represents an intense research topic with the aim to identify novel therapeutic agents and improved treatment schedules. Despite recent advances in androgen depletion therapy, castrate-resistant disease eventually develops in majority of patients. Recent studies proposed that upregulation of receptor tyrosine kinases (RTK), particularly deregulated EGFR signalling, is implicated in the acquisition of an androgen-independent state in PC (Traish & Morgentaler, 2009). However, targeted therapies against the EGFR system in PC have been disappointing (Trotman et al, 2003). Such discrepancies may be explained by complex regulatory mechanisms for the EGFR system and its downstream signalling cascade.

EGFR (HER-1) is a member of the ErbB family, which also consists of HER-2, -3 and -4. There are several reports indicating that ErbB family members contribute to PC progression (Fritzsche et al, 2006; Goltsov et al, 2012; Kim et al, 2009). Epidermal growth factor (EGF) binding at the cell surface induces receptor dimerziation and activation of its tyrosine kinase domain, and the subsequent downstream signalling events, including both phosphatidylinositol 3-kinase (PI3K)/AKT and Ras/Raf/MEK pathways, which are pivotal in controlling proliferation and survival (Baluk et al, 2007; Dejana et al, 2007). Concomitantly, upon EGF binding, the receptor–ligand complexes are internalized into endosomal compart-

(1) Beatson Institute for Cancer Research, Glasgow, UK
(2) Institute for Cancer Sciences, College of Medical, Veterinary and Life Sciences, University of Glasgow, UK
(3) Northern Institute for Cancer Research, Medical School, University of Newcastle-upon-Tyne, Newcastle-upon-Tyne, UK
(4) Department of Pathology, NHS Greater Glasgow and Clyde, Glasgow, UK
***Corresponding author:** Tel: +44 141 330 3658; Fax: +44 141 942 6521; E-mail: h.leung@beatson.gla.ac.uk

ments. The primary role of endocytosis was thought to terminate activation of RTKs, and the attenuation of the receptors by endosomal degradation was even proposed to have a tumour suppressor role (Kim et al, 2002a; Zhang et al, 1997). However, several studies revealed that RTKs continuously recruit signalling molecules to the intracellular compartments, maintaining and amplifying its signalling outcome. More recently, clathrin-mediated endocytosis upon EGFR activation appeared to be particularly important for the activation of AKT and MAPK (Kim et al, 2002b). Zwang and Yarden (Zwang & Yarden, 2006) also proposed that the fate of EGFR was determined by the status of the stress kinase p38 MAPK, the activation of which allowed tumour cells to evade chemotherapeutic agents.

EGFR signalling forms a complex signalling network with positive and negative regulators. SPRY protein was first described by Hacohen and colleagues (Hacohen et al, 1998) as an antagonist of fibroblast growth factor (FGF) signalling in *Drosophila*. Sprouty (SPRY) proteins are commonly deregulated in human cancers including melanoma, breast and colon cancer (Faratian et al, 2011; Weber et al, 2007; Woodfin et al, 2007). In PC, we have previously shown that SPRY2, one of the mammalian SPRY orthologues (SPRY 1–4), is epigenetically silenced in almost 70% of primary PC (McKie et al, 2005). SPRY2 is shown to physically interact with several adaptor/regulator proteins downstream of RTKs, including PP2A, Grb2, Braf, Shp2, c-Cbl and GAP1 (Danese et al, 2007). The large number of binding partners for SPRY2 is consistent with its crucial yet complicated role in RTK signalling. Indeed, whether SPRY2 functions as a positive or negative regulator in the EGFR signalling network remains an important question. In addition to its well-reported function as an inhibitor of the RAS/RAF/MEK signalling cascade (Bordoni et al, 2007), Edwin and his colleagues reported that SPRY2 exerts its inhibitory role in the PI3K/AKT signalling pathway through PTEN by enhancing its activation and stability (Edwin et al, 2006). Kim et al (2007) described the involvement of SPRY2 in EGFR trafficking and the consequent inhibition of ERK/MAPK activity. It is worth noting that the interaction between the EGFR/HER system and SPRY2 loss was not examined in their study.

PTEN is among the most commonly mutated genes in human cancer, including PC. Progressive inactivation or loss of PTEN appears to be involved in the development of invasive and metastatic PC. Transgenic mice with PTEN heterozygous deletion targeted to the prostate develop high-grade prostatic intraepithelial neoplasia (PIN), which fails to progress into an invasive phenotype (Mellinghoff et al, 2004). Furthermore, complete loss of PTEN is thought to be a late event and can be considered a critical landmark for progression to aggressive and invasive disease. Indeed, the *Pten null* murine PC model developed invasive adenocarcinoma (Song et al, 2011). This is consistent with the cBio portal data, which revealed that ~24% (25/104) of PC retains PTEN expression albeit at low levels and ~7% (7/104) of cases displayed a homozygous deletion in human PC (cBio Cancer Genomics Portal; Taylor et al, 2010). It is worth noting that as many as 50% (17/37) of metastatic tumours harboured biallelic *Pten* loss.

To date, the functional impact of SPRY2 has been studied using transiently or stably over-expressed SPRY2 in *in vitro* cell models (Kawakami et al, 2009; Rubin et al, 2003). As SPRY2 expression tends to be suppressed in cancer, we set out to investigate the significance of SPRY2 loss in clinical PC as well as in relevant *in vitro* and *in vivo* model systems. Our data uncovered an important signalling cross talk that SPRY2 deficiency has with the EGFR system (RTK) and PTEN haploinsufficiency to drive hyper-activation of PI3K/p-AKT in PC via enhanced RTK trafficking. Furthermore, using a genetically modified (*Nkx CRE Pten*$^{fl/+}$ *Spry2*$^{+/-}$) mouse PC model with an invasive tumour phenotype, PI3K/AKT activation was tested as a potential target for therapy in PC in the context of aberrant PTEN and SPRY2 signalling.

RESULTS

Clinical impact of abnormal SPRY2 and HER2 expression in human PC

SPRY2 expression was characterized in two-independent PC cohorts in the format of tissue microarray (TMA), namely TMA1 and TMA2 (Supporting Information Table 1). TMA1 included 202 cases of PC and 107 cases of benign prostatic hyperplasia (BPH) as controls. Given the regulatory role of SPRY2 in RTK signalling, the expression status of SPRY2 and all four members of the ErbB families (namely HER1–4) were examined. In BPH, both basal and luminal epithelial (Ep) cells generally exhibited low to moderate immunoreactivity for SPRY2 expression (Supporting Information Fig S1). High grade tumours (Gleason grade 5 disease) expressed SPRY2 at lower levels than better differentiated tumours with Gleason grade ≤ 4 (Fig 1A). Patients with suppressed SPRY2 expression were stratified according to the HER paralogue expression status: those patients with HER2-positive disease have significantly poorer survival outcomes when compared with those with HER2-negative disease ($p = 0.014$; Supporting Information Fig S2). None of the other members of the ErbB receptors showed any association with patient outcome (Supporting Information Fig S3). To further validate if simultaneously reduced SPRY2 and upregulated HER2 expression in clinical PC is associated with unfavourable patient survival outcome, expression of SPRY2 and HER2 was studied in TMA2 (209 PC and 30 BPH cases). We were able to confirm that, among patients with reduced SPRY2 expression, over-expression of cytoplasmic HER2 was significantly associated with an unfavourable overall survival outcome ($p = 0.025$; Fig 1B). A similar result was obtained from the cBio Genomic portal: alteration in the *Spry2* gene significantly reduced the disease-free period in PC patients ($p = 0.000056$; Supporting Information Fig S4). Within a single representative tumour, Fig 1C illustrated tumour cells with simultaneous high HER2 and low SPRY2 expression, respectively. Overall, we observed a significant inverse association between SPRY2 and HER2 expression (Fig 1A and Table 1). Taken together, these results revealed abnormal SPRY2 and HER2 expression in human PC progression and prognosis.

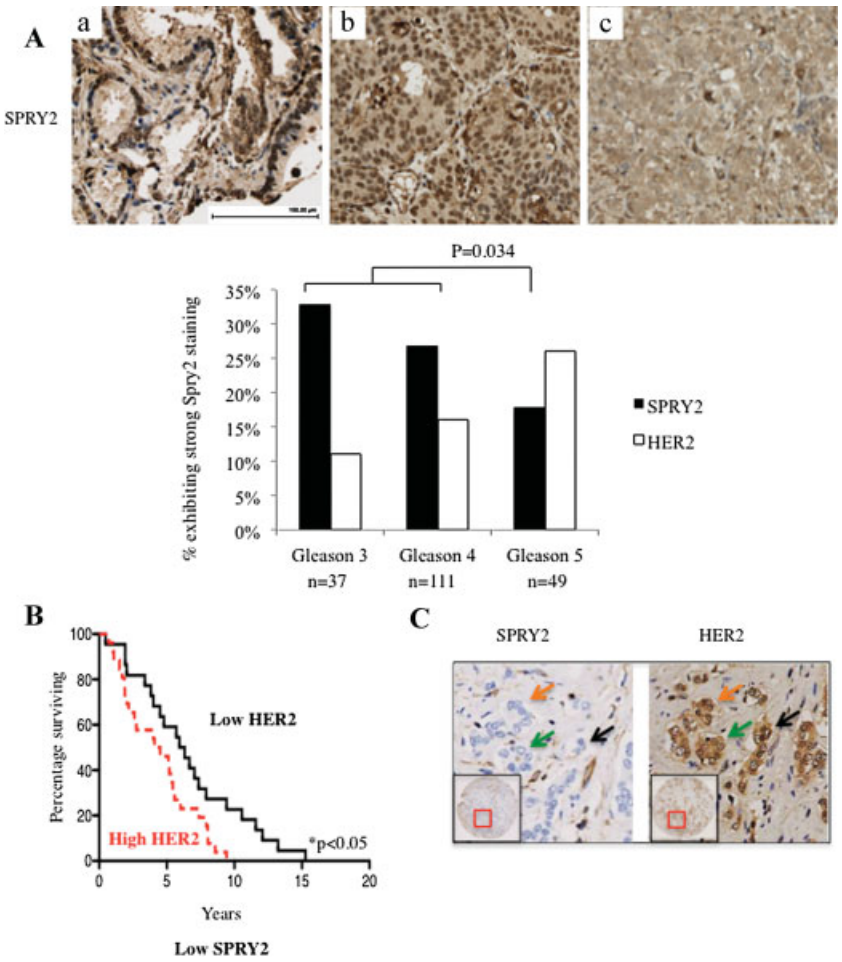

Figure 1. Expression of SPRY2 and HER2 in human PC.

A. Representative images of SPRY2 immunostaining in Gleason grade 3–5 tumours (a–c, respectively; top panels). The percentages of tumours showing strong SPRY2 and HER2 expression (histoscore > 200) were categorized according to the Gleason grades (ranges 1–5): low grade, Gleason grades 1–3 ($n = 37$); intermediate grade, Gleason grade 4 ($n = 111$); high grade, Gleason grade 5 ($n = 49$; $p = 0.034$, $n = 197$ of 202 in TMA1).

B. Human TMA2 was stained for SPRY2 and HER2 immunoreactivity. In patients with low SPRY2, the samples were segregated according to their HER2 expression levels, and Kaplan–Meier curves of disease free survival were plotted ($p = 0.0323$).

C. Representative IHC images from the same case showing, respectively, high HER2 and loss of SPRY2 expression. The arrows indicate the corresponding tissues for HER2 and SPRY2 staining.

Enhanced activation of EGFR and HER2 in SPRY2 KD cells via rapid internalization

To examine the functional significance of SPRY2 loss in prostate carcinogenesis, we generated stable SPRY2 knockdown (KD) clones of PC cell lines: DU145 (clones CL13 and CL61) and PC3 (clones CL1 and CL10) along with their respective non-silencing (Nsi) controls (Supporting Information Fig S5). PTEN has been shown to be essential for SPRY2 to exert its inhibitory effect in EGFR-mediated signalling (Edwin et al, 2006). Hence, we examined the effect of HER2 and EGFR function in SPRY2 KD cell lines derived from DU145 and PC3 cells, which are positive and negative for PTEN expression, respectively. We examined the activation of RTK including HER2, EGFR and HER3 in response to heregulin and EGF. Interestingly, only EGF stimulation led to enhanced activation of HER2 and associated p-AKT in SPRY2 KD cells when compared to the Nsi control. Heregulin activated HER3, but not HER2, in both SPRY2 Nsi control and KD cells (Fig 2A). SPRY2 KD cells responded to EGF treatment with enhanced and sustained activation of HER2 and EGFR, as well as their downstream signalling component p-AKT (Fig 2B).

Table 1. Correlation data from TMA2 on HER2, SPRY2, p-AKT and p-ERK. (HER2(c) = cytoplasmic HER2); range and median of parameters studied

Pearson's correlation	HER2(c)	p-AKT	p-ERK
SPRY2	−0.196 $p = 0.0216$	−0.410 $p = 0.00084$	0.187 $p = 0.0674$ (ns)
HER2(c)	–	0.281 $p = 0.00754$	−0.0997 $p = 0.344$ (ns)
Range	**Minimum**	**Maximum**	**Median**
HER2 (c)	0	300	103
p-AKT	0	245	67
p-ERK	0	300	33
SPRY2	0	107	23

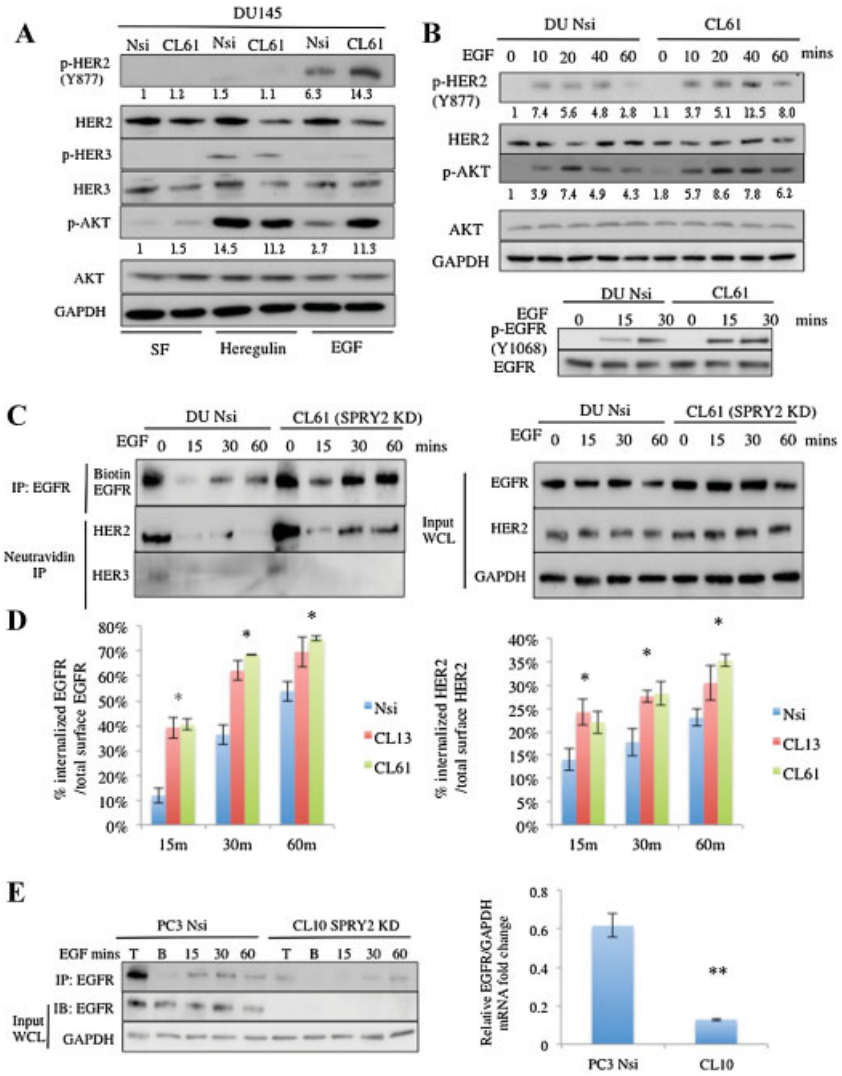

Figure 2. Enhanced activation of EGFR and HER2 in SPRY2 KD cells via rapid internalization.

A. Serum starvation-primed cells were stimulated with heregulin (50 ng/ml) or EGF (20 ng/ml) for 15 min. Whole cell lysates were analysed by Western blotting. The levels of p-HER2 and p-AKT were quantified using Image J and the pixel intensities were normalized to that for Nsi control cells in serum free condition. The relative ratios and representative Western blots are shown ($n = 3$). SF, serum-free; CL, clone.

B. Cells were serum starved overnight and stimulated with EGF for varying durations, as indicated in the figure. The levels of p-HER2, p-AKT and p-EGFR were assayed. GAPDH expression was included as a loading control. The relative ratios of p-AKT and p-HER2 were quantified using Image J and the pixel intensities were normalized to that for Nsi control cells in serum free condition. The relative ratios and representative Western blots are shown ($n = 3$).

C. EGFR in SPRY2 KD and Nsi control DU145 cells was immunoprecipitated. The internalized biotin-EGFR population was detected with Streptavidin–horseradish peroxide. Cells were prepared by labelling surface proteins with NHS-S-S-biotin, followed by stimulation with EGF (for 0, 15, 30 and 60 min) and reduction of surface biotin prior to collection of cell lysates. HER2 and HER3 were detected by IP-western. At time 0 min (control), lysates were obtained without surface biotin reduction. For WCL (whole cell lysate) input, HER2, EGFR and GAPDH were blotted.

D. The percentages of internalized receptors for EGFR and HER2 were quantified and normalized to 'total' surface receptors (at 0 min) in DU145 Nsi control cells and SPRY2 KD clones (CL13 and CL61), respectively. EGF-induced receptor internalization in SPRY2 KD cells was significantly higher than that for Nsi control cells: EGFR internalization, $^{*}p = 0.02$, 0.01 and 0.02 at 15, 30 and 60 min, respectively; HER2 internalization, $^{*}p = 0.02$, 0.01 and 0.03 at 15, 30 and 60 min, respectively. All results are shown as mean values plus or minus (±) s.e.m from three-independent experiments and analysed by student's *t*-test.

E. Left panel: In parallel to internalization assay on PC3 cells, IP was performed as in Fig 2C, and lysates were blotted for biotin-EGFR with Streptavidin–horseradish peroxide. WCL inputs were collected and immunoblotted for EGFR and GAPDH. T, total surface EGFR; B, blank control from samples with reduced surface biotin, without EGF stimulation, i.e. no internalization. Right panel: EGFR mRNA levels were quantified in PC3 Nsi control and SPRY2 KD cells. The fold change in EGFR expression was normalized to GAPDH as a control ($^{**}p = 0.009$, all results are shown as means ± SD from three-independent replicates and analysed by student's *t*-test).

Upon ligand binding, EGFR is involved in a series of trafficking events, which ultimately regulate its signal amplification and propagation. We therefore investigated the intracellular distribution of EGFR using fluorescence microscopy. In unstimulated cells, EGFR was predominantly localized to cell surface. Following EGF stimulation, internalized EGFR co-localized with EEA1-positive early endosomes in both Nsi control and SPRY2 KD cells. SPRY2 KD DU145 cells had more sustained EGFR localization to the early endosomes than the Nsi control cells at both 20 and 30 min (Supporting Information Fig S6).

To characterize the molecular basis of EGFR trafficking to the early endosomes, the internalization kinetics of EGFR in SPRY2 KD DU145 cells was studied. In the presence of primaquine (a receptor recycling inhibitor), immuno-precipitation for NHS-S-S-biotin-labelled EGFR showed increased levels of intracellular EGFR and HER2 in SPRY2 KD DU145 cells treated with EGF for 15, 30 and 60 min, an observation not seen for HER3 (Fig 2C). This was further supported by pooled and quantified data showing the percentage of cell surface EGFR and HER2 that were endocytosed in SPRY2 KD DU145 clones (Fig 2D). Increased internalization and accumulation of EGFR in SPRY2 KD cells was also studied using the NHS-S-S-biotin internalization assay in an ELISA format. We detected ~20% more intracellular EGFR in SPRY2 KD cells (Supporting Information Fig S7). In contrast to the PTEN-proficient DU145 cells, reduction in SPRY2 expression reduced EGFR levels in the PTEN-null PC3 cells (Fig 2E). Pooled quantitative data on EGFR protein levels in PC3 Nsi and SPRY2 KD clones from three-independent experiments confirmed that suppressed SPRY2 expression diminished EGFR protein levels (Supporting Information Fig S8). To further evaluate this observation, EGFR mRNA expression in PC3 SPRY2 KD and Nsi control cells was assayed using qRT-PCR. EGFR mRNA expression in PC3 SPRY2 KD cells was significantly reduced when compared to the corresponding Nsi control cells (Fig 2E). Furthermore, ectopic expression of PTEN in PC3 SPRY2 KD clones at least partially rescued EGFR expression at the protein level (Supporting Information Fig. S9). Indeed, PTEN siRNA transfection in DU145 cells confirmed that simultaneous loss of PTEN and SPRY2 led to reduced EGFR and HER2 expression (Supporting Information Fig S10). Altogether, loss of SPRY2 promotes rapid internalization and sustained accumulation of intracellular EGFR and HER2 in response to EGF stimulation in a PTEN-dependent manner.

Loss of SPRY2 mediates EGF-driven proliferation in a PTEN-dependent manner

Using *in vitro* functional assays, we observed significantly enhanced EGF-mediated proliferation and invasion in SPRY2 KD DU145 cells (Fig 3A and C). In contrast, in EGF-treated SPRY2 KD PC3 cells, proliferation was unaffected (Fig 3B) while invasion was suppressed (Fig 3D). We hypothesized that enhanced EGF-mediated proliferation and invasion observed in SPRY2 KD DU145 cells were due to sustained EGFR/HER2 signalling resulting from abnormal trafficking in a PTEN-dependent manner. Indeed, knocking down PTEN expression in SPRY2 KD DU145 cells impaired EGF-induced invasion and abolished the observed upregulation of proliferation. Interestingly, Nsi control cells showed an increase in EGF-mediated invasion and proliferation upon PTEN KD (Fig 3E and F). Data from DU145 SPRY2 KD cells with siRNA-mediated PTEN KD was consistent with that from (PTEN null) PC3 SPRY2 KD cells (Fig 3B and D). Restoration of PTEN significantly increased proliferation in SPRY2 KD PC3-derived clones (Fig 3G). Of note, PC3 cells with transfected PTEN expression showed a similar growth pattern when compared with the PTEN-positive DU145 cells (Fig 3A). Furthermore, the levels of p-PTEN (Ser380) and total PTEN expression only showed very minor changes in SPRY2 KD DU145 cells. Hence, in DU145 cells, the impact of SPRY2 loss-mediated EGFR signalling was likely not related to changes in PTEN expression (Supporting Information Fig S11). Similarly, suppression of PTEN expression by siRNA treatment did not influence SPRY2 expression: PTEN siRNA transfection in DU145 SPRY2 KD cells did not affect SPRY2 expression with consistently low SPRY2 levels when compared to the control Nsi cells (Supporting Information Fig S10).

In SPRY2 KD PC3 cells, we observed no induction of proliferation upon EGF stimulation when compared to the control Nsi cells (Fig 3B). This contrasts with the significant induction of proliferation in the PTEN proficient DU145 cells and the PC3 cells with transfected PTEN expression. To further test the relationship of PTEN and SPRY2 status on the regulation of proliferation, LNCaP cells, a human PC cell line deficient for both PTEN and SPRY2 expression, were studied. In the absence of PTEN expression, transfected SPRY2 expression did not influence cell proliferation nor p-AKT activation (Supporting Information Fig S12), thus recapitulating data from PC3 cells. We then investigated 22Rv1 cells (PTEN- and SPRY2-positive). In 22Rv1 cells, similar to DU145 cells, stable loss of SPRY2 significantly enhanced cell growth as well as upregulated EGFR/HER2 phosphorylation along with PI3K/AKT activation as their downstream signalling partners (Supporting Information Fig S13). Consistent with these observations and in contrast to the earlier observation in Fig 1B, Kaplan–Meier analysis for PTEN-negative tumours in our clinical TMA revealed no association between HER2 expression and disease-free survival (Supporting Information Fig S3d). Taken together, loss of SPRY2 cooperates with EGF stimulation and enhances proliferation and invasion in a PTEN-dependent manner.

PI3K/p-AKT is a key signalling pathway for SPRY2 loss-mediated effects

Downstream signalling following EGF stimulation in PTEN-proficient SPRY2 KD DU145 cells was examined using the Human Phospho-Kinase Array. Cells were serum starved overnight and stimulated with EGF for 15 min. Among the 46 phospho-kinases profiled, both PI3K/AKT and MAPK were activated upon EGF stimulation (Supporting Information Fig S14). Upregulation of p-ERK and p-AKT in SPRY2 KD DU145 cells was further validated in Western blots following 15 and 30 min of EGF stimulation (Fig 4A). Enhanced p-AKT activation was observed following EGF and not heregulin treatment in SPRY2 KD cells compared to the respective Nsi control cells (Figs 4A and 2A). In contrast, upon EGF stimulation, the PTEN

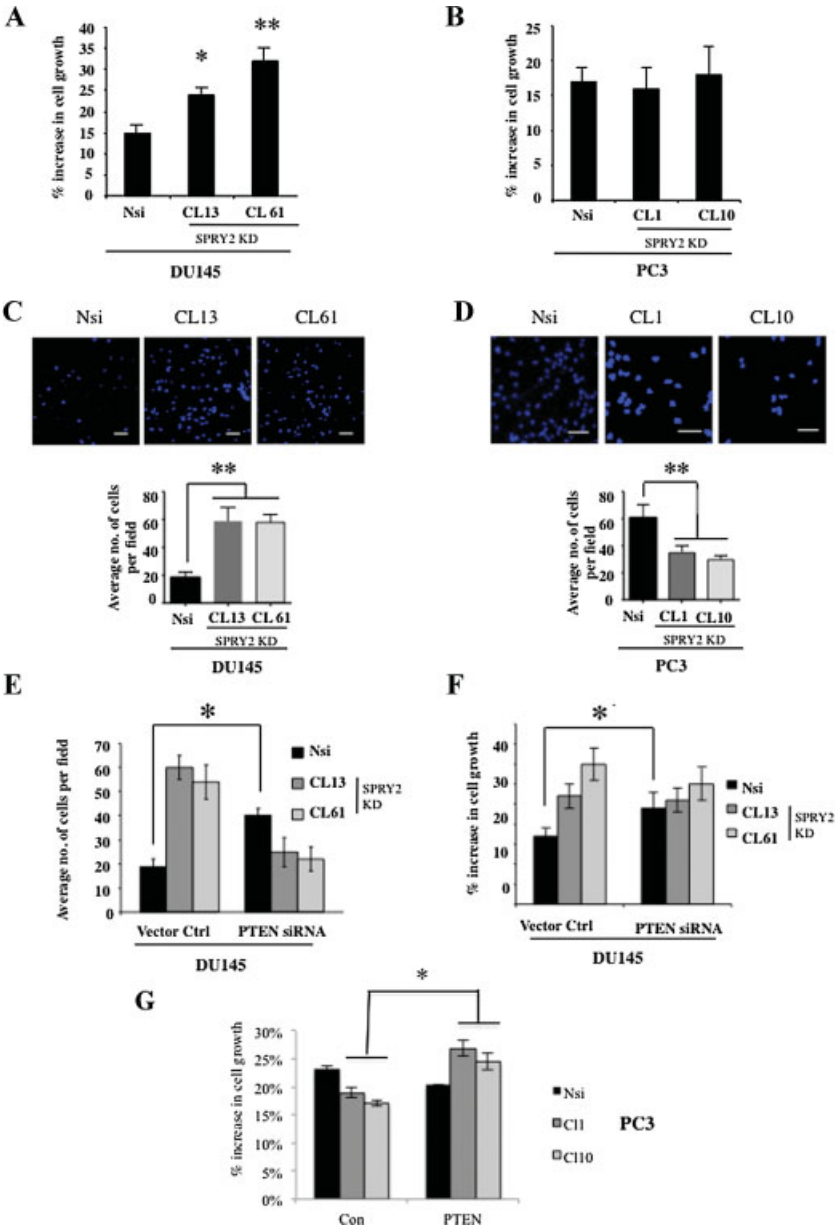

Figure 3. Loss of SPRY2 mediates EGF driven proliferation in a PTEN-dependent manner.

A,B. Serum-starved SPRY2 KD DU145 (panel **A**) and PC3 (panel **B**) cells were treated with EGF (20 ng/ml for 48 h) in a WST-1 growth assay. For DU145-derived cells, SPRY2 KD DU145 showed enhanced EGF induced growth: $^{*}p = 0.02$ and $^{**}p = 0.007$ for Cl13 and Cl61, respectively ($n = 3$). The percentage of increase in cell proliferation was derived from data normalized to serum free and EGF-free conditions for the respective cell line. All results are shown as means plus or minus (±) SD from three-independent experiments and student *t*-tests were performed.

C,D. Invasiveness of DU145- and PC3-derived SPRY2 KD and Nsi cells was quantified in the presence of EGF as a chemoattractant for 8 h. Cells were stained by DAPI and visualized using confocal microscope. $^{**}p = 0.002$ for DU145 SPRY2 KD cells with increased invasion and $^{**}p = 0.001$ for PC3 SPRY2 KD cells with reduced invasion ($n = 3$). In absence of EGF as chemo-attractant, we observed negligible numbers of invading cells. All results were shown as means ± SD (Scale bars = 100 μm). One-way ANOVA was performed.

E,F. SPRY2 KD and Nsi control DU145 were transfected with PTEN siRNA. The average numbers of invading cells through the matrigel plug are shown in panel **E**. For the WST-1 assay (**F**), data from individual cells were normalized to that of serum- and EGF-free medium control and the percentage increase in cell growth is shown. All results were shown as means ± SD ($^{*}p = 0.04$ for invasion assay and $^{*}p = 0.03$ WST-1 assay, $n = 3$ (student's *t*-test).

G. PTEN is ectopically expressed in PC3 Nsi control and SPRY2 KD cells. Cell growth was assayed and quantified using WST-1 assay ($^{*}p = 0.011$, $n = 3$, one-way ANOVA). The percentage of increase in cell proliferation was derived from data normalized to serum- and EGF-free conditions for each cell line. All results were shown as means ± SD from three-independent replicates.

null SPRY2 KD PC3 cells showed significantly reduced p-AKT activation, while activation of p-ERK was enhanced. In addition, we observed enhanced JNK phosphorylation, which is downstream of PI3K/AKT and has been implicated to promote proliferation and angiogenesis in PC (Slack et al, 2005). It is interesting that both MEK1/2 and the downstream ERK1/2 are activated in SPRY2 KD DU145 cells (Supporting Information Fig S15). Of note, activation of the stress MAP kinase p38 was also enhanced by EGF in SPRY2 KD cells (Supporting Information Fig S15). Considering the functional differences between DU145 and PC3 cells observed in Fig 3, we reasoned that loss of SPRY2 activates downstream signalling cascades in a PTEN-dependent manner to regulate cell growth and invasion.

Our working model is that loss of SPRY2 interacts with abnormal intracellular signalling to drive PI3K/AKT hyper-activation-mediated prostate carcinogenesis. Therefore, to test the significance of PI3K/AKT signalling, SPRY2 KD DU145 cells were treated with the PI3K inhibitor LY294002 and studied in proliferation and invasion assays. SPRY2 KD DU145 showed significantly reduced growth and invasion in the presence of LY294002. In contrast, the MEK inhibitor PD098059 did not have any effects (Fig 4B and C). It is worth noting that LY294002 treatment did not alter either SPRY2 or PTEN protein levels (Fig 5G). Furthermore, to test the functional significance of internalized EGFR signalling (including those molecules localized to the early endosomes), dynasore, a cell permeable inhibitor of dynamin, was used to inhibit clathrin-mediated endocytosis. As expected, dynasore inhibited EGFR endocytosis in both control and SPRY2 KD cells (Fig 4D). As a control, in the absence of EGF stimulation, EGFRs are predominantly detected

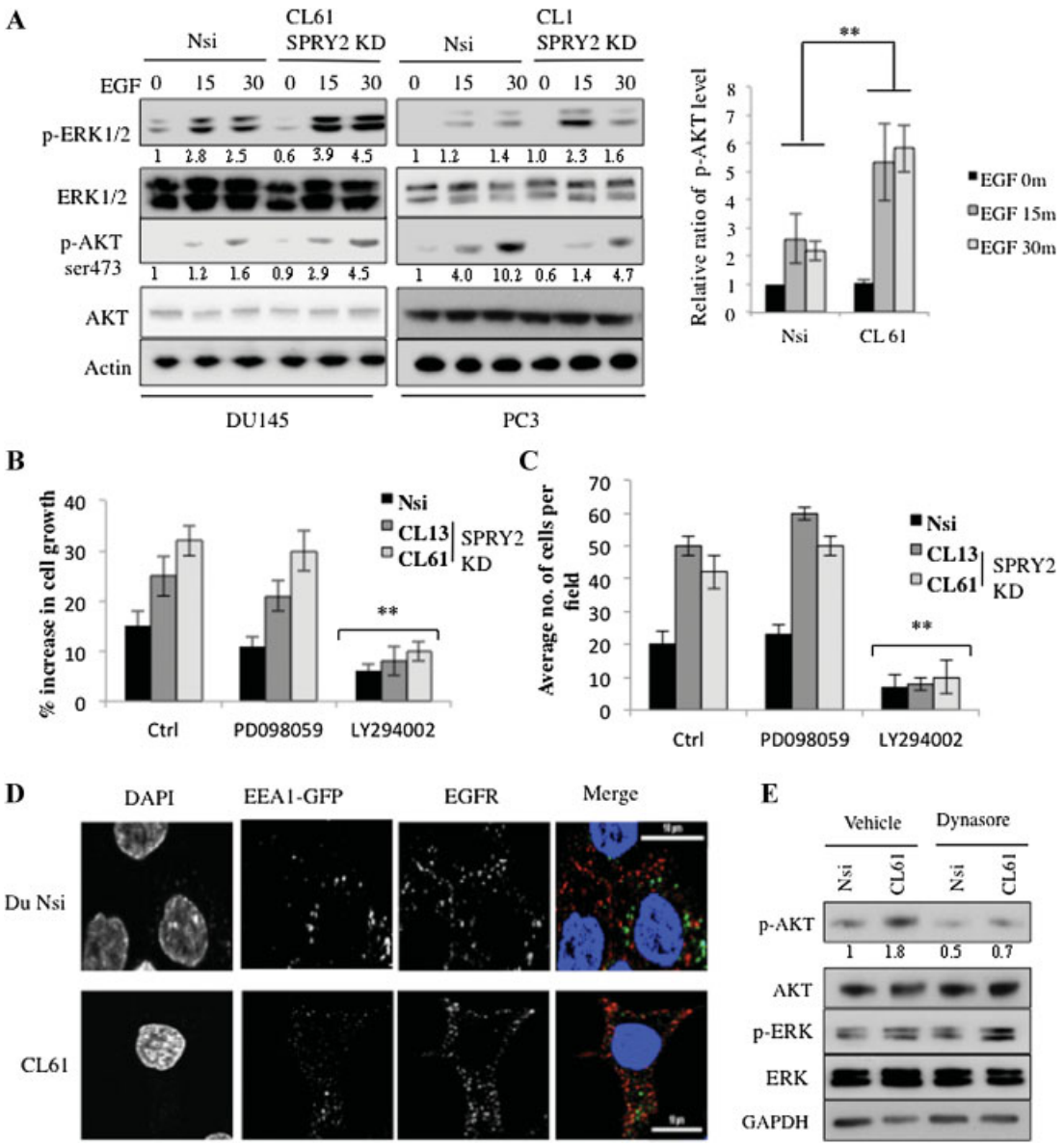

Figure 4. PI3K/p-AKT is a key signalling pathway for SPRY2 loss-mediated effects.

A. DU145- and PC3-derived Nsi control and SPRY2 KD cells were serum starved overnight and stimulated with EGF (20 ng/ml) for 15 and 30 min. Whole cell lysates were assessed using Western blotting. Actin was used as a loading control. Phosphorylation levels were quantified using Image J and the pixel intensities were normalized to that for Nsi control cells in serum- and EGF-free conditions. The relative ratios and representative Western blots are shown. Right panel shows the average relative ratios of p-AKT level in DU145 control Nsi and SPRY2 KD cells following EGF stimulation normalized to the respective serum free control cells ($^{**}p = 0.008$, $n = 3$, one-way ANOVA), the results are shown as means ± s.e.m from three-independent experiments.

B. SPRY2 KD and Nsi control DU145 cells were treated with PD098059 (10 μM), LY294004 (10 μM) or DMSO as a vehicle control, and analysed for cell proliferation by the WST-1 assay ($^{**}p = 0.001$, one-way ANOVA). The percentage of increase in cell growth was derived from data normalized to serum free control without EGF stimulation. All results are shown as means ± SD from three-independent replicates.

C. Invasiveness of SPRY2 KD and Nsi DU145 cells was quantified in the presence of EGF as a chemoattractant after 8 h incubation ($^{**}p = 0.002$, $n = 3$, one-way ANOVA). The average number of cells observed per field is shown. All results were shown as means ± SD.

D. EEA1-GFP transfected cells were treated with dynasore (5 μM) in the presence of EGF. EGFR, GFP (EEA1-GFP) and DAPI were visualized (scale bar = 10 μm; Blue for DAPI staining, green for GFP-positive EEA1 staining and red for EGFR).

E. Cells were treated with dynasore (5 μM) in the presence of EGF. Whole cell lysates were collected and analysed by Western blotting as indicated. GAPDH was used as a loading control. p-AKT level was quantified using Image J and the pixel intensities were normalized to that for Nsi control cells in vehicle control condition. The average relative ratios and representative Western blots are shown.

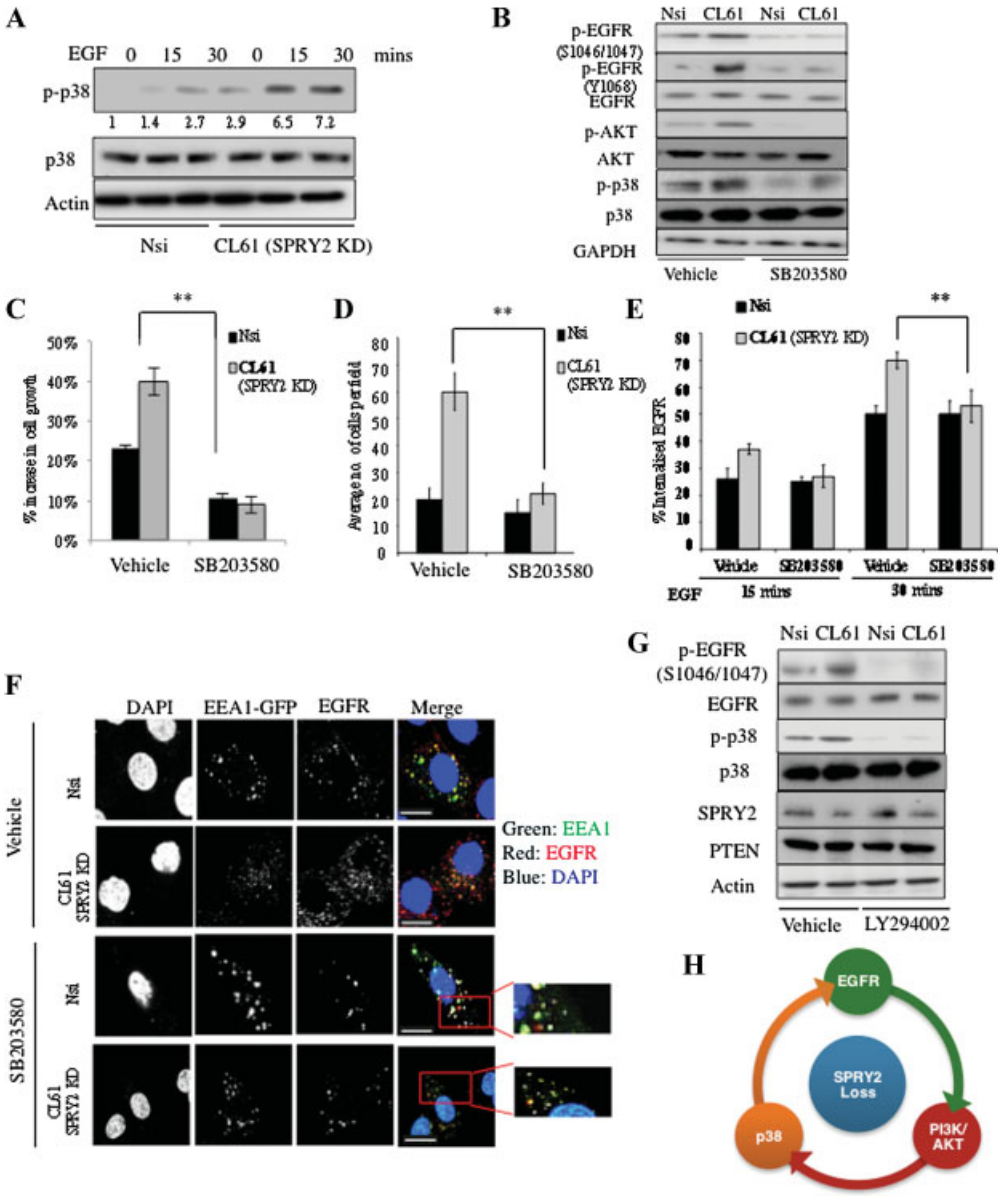

Figure 5. SPRY2 KD increases EGFR endocytosis via p38 and PI3K.

A. Serum starvation-primed SPRY2 KD and Nsi control DU145 cells were stimulated with EGF (20 ng/ml) for 15 min, and cell lysates were Western blotted with indicated antibodies. Actin was used as a loading control. p-p38 level was quantified using Image J and the pixel intensities were normalized to that for Nsi control cells in serum free condition. The relative ratios and representative Western blots are shown.

B. SPRY2 KD and Nsi control DU145 cells were pre-treated with either SB203580 (10 μM) or DMSO (vehicle control) for 6 h prior to EGF treatment (20 ng/ml and 15 min). Western blot analysis was carried out as in panel **A**.

C. EGF (48 h) mediated cell growth in DU145 derived cells was assayed with or without p38 inhibitor (SB203580, 10 μM) treatment ($^{**}p = 0.0003$, $n = 3$, student's *t*-test). The results were shown as means ± SD. The percentage of increase in cell proliferation was derived from data normalized to serum free control for each cell line.

D. EGF (8 h, 20 ng/ml) mediated invasion in DU145 derived cells was assayed with or without p38 inhibitor (SB203580) pre-treatment ($^{*}p = 0.009$, $n = 3$, student's *t*-test). The results are shown as means ± SD.

E. Internalized EGFR following EGF stimulation (15, 30 min) were quantified in SPRY2 KD and Nsi control DU145 cells with or without p38 inhibitor (SB203580) treatment ($^{**}p = 0.003$, $n = 3$, student's *t*-test). The results were shown as means ± SD. The percentage of internalized EGFR was normalized to the total surface EGFR before EGF treatment.

F. Representative images of SPRY2 KD and Nsi control DU145 cells following EGF (20ng/ml, 30 min) stimulation with SB203580 or DMSO control. Merged images show EEA1-GFP (green), EGFR (red), and nuclei (blue; Scale bar = 10 μm).

G. SPRY2 KD and Nsi control DU145 cells were pre-treated with either LY294004 (10 μM) or DMSO for 6 h, and then stimulated by EGF (15 min, 20 ng/ml). Cell lysates were then analysed by Western blotting.

H. Schematic representation showing the positive feedback loop between EGFR, PI3K and p38 in SPRY2 loss background.

at the cell surface following dynasore treatment (Supporting Information Fig S16). Significantly, EGF-induced activation of p-AKT in SPRY2 KD cells was abolished, confirming the importance of endosomal EGFR in promoting PI3K/AKT signalling (Fig 4E). This contrasts with the absence of effects on p-ERK following dynasore treatment.

SPRY2 KD increases EGFR endocytosis via p38 and PI3K

P38 is a key regulator of EGFR and can phosphorylate EGFR at Ser-1046/1047, which is closely linked to internalization of the receptor (Nishimura et al, 2009). Furthermore, Zwang and Yarden proposed that chronic activation of p38 facilitates accumulation of EGFR in the endosomal compartments and aids tumour cell survival (Zwang & Yarden, 2006). Elevated phospho-p38 level in SPRY2 KD cells was observed in the Human Phospho-kianse array (Supporting Information Fig S15). Furthermore, enhanced phosphorylation of p38 and EGFR (Ser-1046/1047) was observed in EGF stimulated SPRY2 KD DU145 cells (Fig 5A and B). To examine the role of p38 in SPRY2 KD-associated EGFR internalization and signalling, cells were treated with the p38 inhibitor SB203580. Pharmacological suppression of p38 function with SB203580 abolished activation of AKT following EGF stimulation (Fig 5B) and significantly reduced both cellular growth and invasion (Fig 5C and D). In addition, siRNA transfection specifically targeted against p38 significantly reduced both proliferation and invasion of SPRY KD cells (Supporting Information Figs S17 and S18). SB203580 also reduced EGFR internalization in SPRY2 KD cells (Fig 5E), which is mediated via its effect on EGFR phosphorylation at S1046/1047 (Fig 5B). Inhibition of S1046/47 resulted in reduction of EGFR trafficking, consequently abolished activation of EGFR and inhibited upregulation of phosphorylation at tyrosine residues including Y1068. Specifically, co-localization between EGFR and early EEA1-positive endosomes was significantly reduced in SPRY2 KD cells upon p38 inhibition (Fig 5F). p38-specific effects of SB203580 were assessed using the level of ATF2 phosphorylation, which is a direct target of p38. Phosphorylation of ATF2 was suppressed by SB203580 in both Nsi and SPRY2 KD DU145 cells (Supporting Information Fig S19). Furthermore, we investigated the relationship between PI3K/AKT and p38 signalling. The PI3K inhibitor LY294002 abolished phosphorylation of both p38 and EGFR (S1046/1047) in EGF-treated DU145 KD CL61 and control cells (Fig 5G). Collectively, these results indicate that SPRY2 loss results in activation of PI3K and its downstream effector p38 to promote EGFR trafficking and signalling, thus forming a positive feedback loop (Fig 5H).

Loss of SPRY2 and PTEN results in aggressive PC in a mouse model

Based on the data from our *in vitro* studies and human TMA expression analyses, a *Spry2*- and *Pten*-heterozygous mouse model was generated to investigate the *in vivo* impact of SPRY2 and PTEN on prostate carcinogenesis. *Nkx* $Pten^{fl/+}$ $Spry2^{+/-}$ mice were generated and the prostate tissue was harvested from mice around 10–12 months old. Consistent with previous reports (Shen & Abate-Shen, 2010), $Pten^{fl/+}$ mice developed pre-malignant PIN lesions in their prostate glands, while combined haplo-insufficiency of *Spry2* and *Pten* resulted in aggressive prostate tumours (12 out of 12 mice at 10–12 months). Figure 6A shows loss of glandular structure and cancer cells infiltration into surrounding areas. As expected, there were more Ki67-positive cells in $Pten^{fl/+}$ $Spry2^{+/-}$ relative to $Pten^{fl/+}$ $Spry2^{+/+}$ prostate, indicating increased proliferation (Fig 6A). Consistent with their genotype, reduced SPRY2 immunoreactivity was observed in $Pten^{fl/+}$ $Spry2^{+/-}$ prostate tumours when compared to the prostates from wild type and $Pten^{fl/+}$ $Spry2^{+/+}$ mice (Fig 6B). As loss of PTEN is expected to lead to PI3K/AKT activation, both $Pten^{fl/+}$ $Spry2^{+/+}$ and $Pten^{fl/+}$ $Spry2^{+/-}$ showed enhanced AKT activation. It is worth noting that simultaneous haplo-insufficiency of *Pten* and *Spry2* resulted in relatively higher levels of p-AKT with predominantly plasma membrane staining (Fig 6C). In contrast, p-ERK2 immunoreactivity was restricted to focal area within the $Pten^{fl/+}$ $Spry2^{+/}$ prostate tumours (Fig 6C). These results suggest that concomitant haplo-insufficiency of the tumour suppressor genes *Pten* and *Spry2* leads to activation of PI3K/AKT in driving aggressive prostate carcinogenesis *in vivo*.

$Pten^{fl/+}$ $Spry2^{+/-}$-driven prostate cancer is highly responsive to PI3K inhibition

The significance of SPRY2 loss-induced AKT activation was examined using the potent PI3K inhibitor PI103 (Carracedo et al, 2011). First, using DU145 SPRY2 KD (CL61) cells *in vitro*, PI103 treatment drastically suppressed growth of SPRY2 KD cells; the fold change was significantly higher than that observed for the Nsi control cells (Supporting Information Fig S20). Next, $Pten^{fl/+}$ $Spry2^{+/-}$ mice harbouring prostate tumours were treated with PI103, following which the prostatic tumour showed reduced proliferation with significantly fewer Ki67-positive cells (Fig 7A). Using a combination of Western blotting and immunohistochemistry (IHC) experiments, p-AKT levels were found to be reduced following PI3K inhibition (Fig 7B and C), while SPRY2 expression was not altered (Supporting Information Fig S21). Supporting our working model (Fig 5H), both EGFR and HER2 expression were significantly reduced upon inhibition of PI3K function (Fig 7B). Even in the presence of increasing tumour bulk and invasion, these tumours retained their PTEN expression as shown by Western blot analysis and IHC staining. PTEN immunoreactivity was observed at high level in lymphocytes (Ly) and at relatively lower level in the Ep cells (Fig 7C and Supporting Information Fig S22), thus excluding the involvement of *de novo* loss of the remaining *Pten* allele. Prostatic lesions in these animals following PI103 treatment were noticeably cystic (Fig 7B, lower panels), compared to the solid nature of the tumours in control treated animals. Hence the lymph node status was used to assess the impact of PI3K inhibition in PC progression. In the cohort of $Pten^{fl/+}$ $Spry2^{+/-}$ mice studied, 3 of 4 animals treated with vehicle control developed metastatic lymph node lesions with evidence of AR expression (Fig 7D and Supporting Information Fig S23). However, none of the four PI103-treated animals developed metastatic nodal disease ($p = 0.025$). Furthermore, p-ERK1/2 expression was similar between treated and untreated

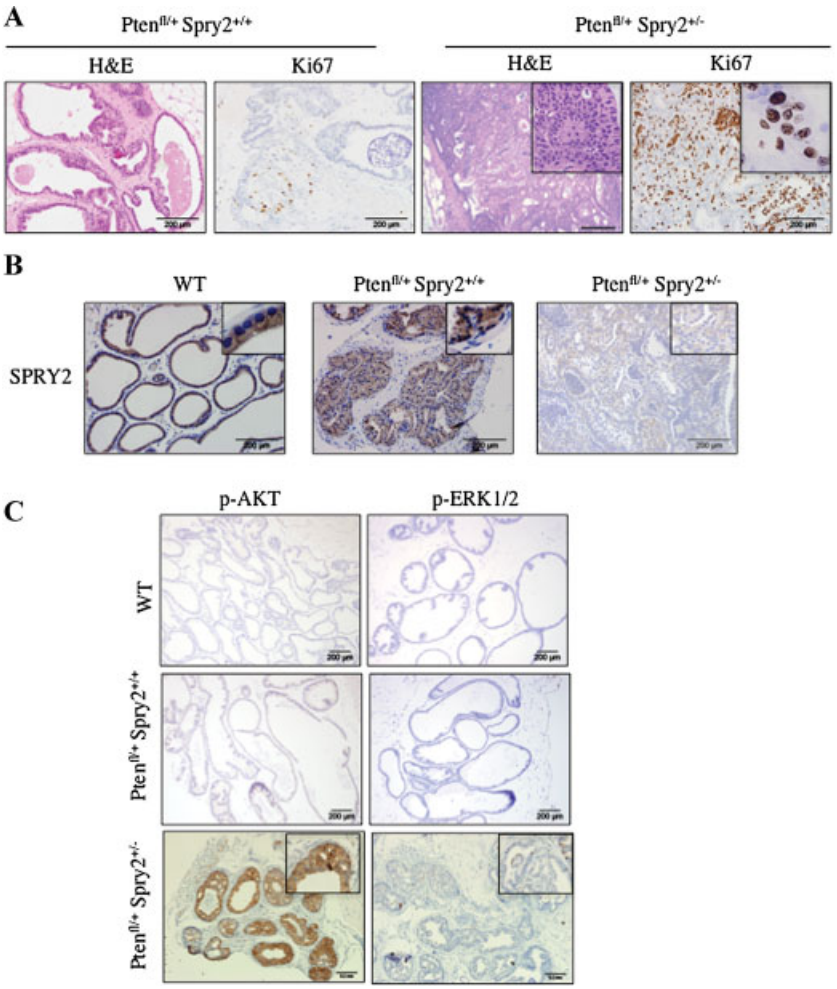

Figure 6. Loss of SPRY2 and PTEN results in aggressive PC in mouse model.

A. Representative tissue sections of H&E and Ki67 staining are shown. Prostate tissues were collected from *Pten*$^{fl/+}$ *Spry2*$^{+/+}$ and *Pten*$^{fl/+}$ *Spry2*$^{+/-}$ mice (scale bar = 200 μm). Inserts show representative area at higher magnification

B. Representative images of SPRY2 expression in prostatic tissue sections from wild type (WT), *Pten*$^{fl/+}$ *Spry2*$^{+/+}$ and *Pten*$^{fl/+}$ *Spry2*$^{+/-}$ mice are presented (scale bar = 200 μm). Insert shows representative area at higher magnification.

C. Representative IHC images of p-AKT and p-ERK1/2 staining in prostatic tissue sections from wild type (WT), *Pten*$^{fl/+}$ and *Pten*$^{fl/+}$ *Spry2*$^{+/-}$ mice are shown (scale bar = 200 μm). Inserts provide magnified view of area of interest.

prostatic tissues (Supporting Information Fig S24). Enhanced apoptosis as illustrated by pyknotic and roughly rounded nuclei in TUNEL assay was also observed in PI103-treated tumours (Supporting Information Fig S25). In summary, enhanced PI3K/AKT signalling significantly contributes to prostate carcinogenesis driven by SPRY2 and PTEN loss.

DISCUSSION

In our previous studies, we showed evidence of epigenetic silencing of *SPRY2* in PC (McKie et al, 2005). In addition, recent human genomic profiling data also revealed frequent abnormalities in signalling molecules such as EGFR, SPRY2, and PTEN (Taylor et al, 2010). For the first time, our findings uncovered a critical feedback system, whereby SPRY2 loss leads to PI3K/AKT activation coupled to activation of p38 MAPK in driving EGFR trafficking and its sustained intracellular localization. The observed PI3K/AKT activation is PTEN-dependent and is at least in part mediated by enhanced phosphorylation of PTEN (Edwin et al, 2006). Our *in vivo* studies on a mouse prostate model and clinical PC specimens provided additional evidence for a key role of PI3K/AKT in prostate carcinogenesis, particularly in the context of SPRY2 loss. Hence, our hypothesis is that PC with SPRY2 loss, partial inactivation of PTEN, and HER2 expression are particularly susceptible to PI3K/AKT-targeted therapy. This will form the basis of our future clinical trial design. In addition, further reduction or complete loss of PTEN along with impaired SPRY2 expression resulted in RTK (EGFR and HER2) degradation, thus rendering the cells insensitive to therapies targeting these receptors. Consistently with our findings, Chandarlapaty et al (2011) also reported enhanced expression of growth factor receptors (such as EGFR and HER2) upon AKT inhibition. Furthermore, Carver et al (2011) have previously shown that PTEN-deficient prostate tumours and PC cells have decreased HER2/3 expression. Hence, besides PTEN, our finding that additional loss of another negative regulator, namely SPRY2, also decreased the expression of EGFR and HER2. Taken together, this suggests that expression of growth factor receptors is dependent on the presence of negative regulators, and highlights the importance of feedback inhibition between RTK signalling cascades and growth factor receptor expression. The SPRY2 KD PC3 cells (CL10) showed increased ERK activation.

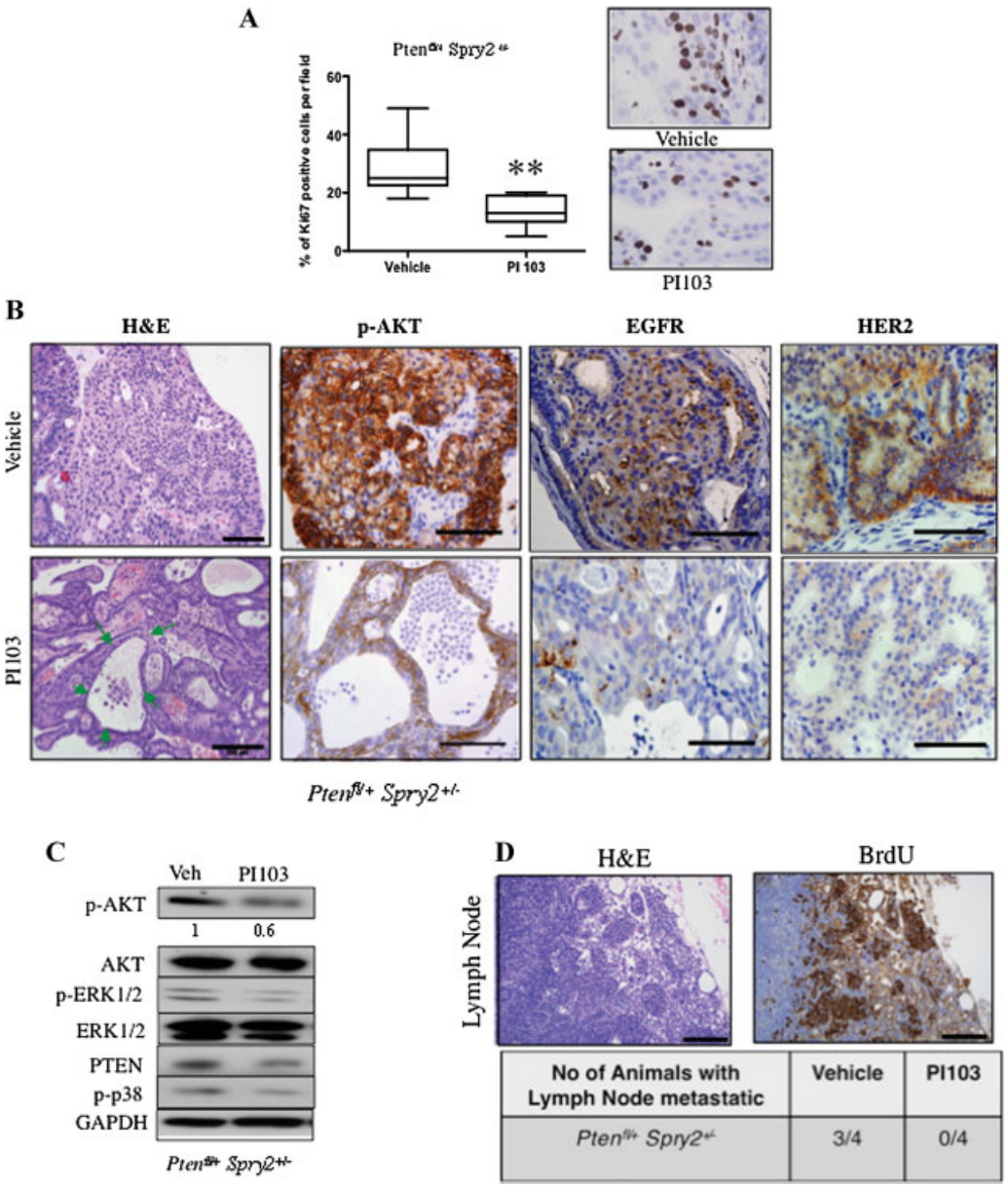

Figure 7. PI3K inhibitor reduces proliferation in *Pten*$^{fl/+}$ *Spry2*$^{+/-}$ tumour *in vivo*.

A. *Pten*$^{fl/+}$ *Spry2*$^{+/-}$ mice (10–12 months) were treated with vehicle or PI103 (50 mg/kg) for 4 weeks, and the prostates were examined. The percentage of prostatic Ep cells per field positive for Ki67 expression was quantified and illustrated in the images ($^{**}p = 5.464E{-}05$, $n = 4$, student's *t*-test). The results are shown as means ± s.e.m.

B. Representative tissue sections of H&E and immunostaining of indicated antibodies are shown (scale bar = 200 μm).

C. Representative Western blots of protein extracts on prostatic tissues from *Pten*$^{fl/+}$ *Spry2*$^{+/}$ mice (10–12 months) following treatment with PI103 (50 mg/kg) or vehicle control. GAPDH was included as a loading control. p-AKT level was quantified using Image J and the pixel intensities were normalized to that for Nsi control cells in serum free condition. The relative ratios and representative Western blots are shown.

D. Enlarged lymph nodes were collected and representative images of H&E and BrdU staining were shown (scale bar = 200 μm). The table summarizes the incidence of detectable lymphatic metastasis following the two treatments.

Hence, it is plausible that this activated ERK may be involved in decreased EGFR and HER2 expression via feedback inhibition. However, the exact mechanism by which the negative regulators (PTEN and SPRY2) regulate the expression of growth factor receptors needs further elucidation.

The binding of ligands to EGFR also leads to homo- and hetero-dimerization with members of the HER kinase family (Voeller et al, 1997). Interestingly, we observed the involvement of HER2, but not HER3, in the flow of EGFR trafficking, further contributing to enhanced RTK-mediated intracellular signalling.

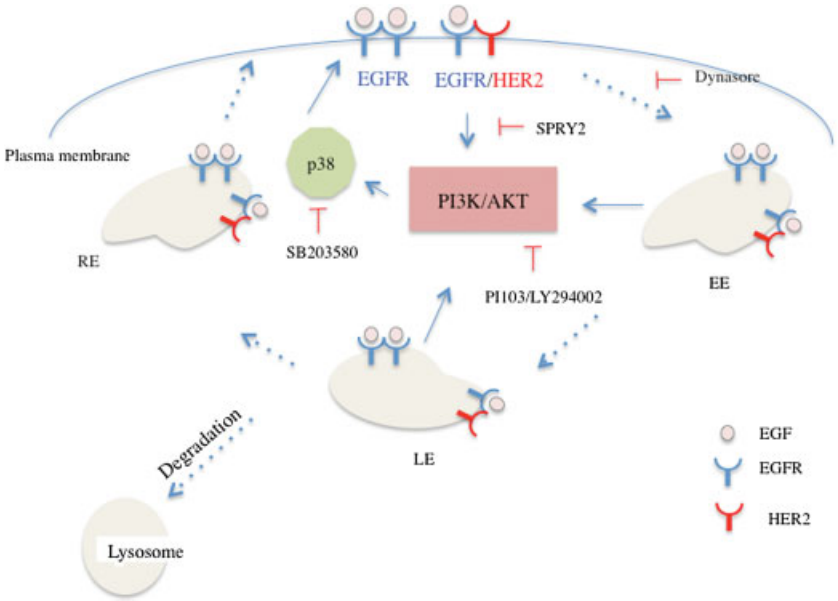

Figure 8. Schematic summary of the analysed pathways. Diagram presents the signalling network of EGFR and HER2 as homo- or hetero-dimers at plasma membrane upon ligand binding and their fate through the endocytic compartments. Loss of SPRY2 accelerates the trafficking of both EGFR and HER2 through early endosome (EE), late endosome (LE) and recycling endosome (RE), thus providing a basis for EGFR and HER2 to continuously signal and to maintain amplified downstream effects. Solid arrows indicate relevant downstream targets of RTK, and dotted arrow shows the trafficking routes of receptors within the cytoplasmic compartments.

The stress-inducible kinase p38 can mediate phosphorylation of EGFR to evade receptor degradation and to produce sustained and enhanced signalling at the endosomes. Consistent with our findings, Zwang and Yarden (Zwang & Yarden, 2006) also postulated that activation of p38 by chronic stress in tumours (either intrinsically or induced by treatments including cytotoxic drugs) can enhance EGFR localization to the endosomes with a pro-survival effect. In summary, profiling tumours for their SPRY2, ErbB and PTEN status can be considered as a rationale for selecting the PC patient cohort for future targeted therapy, including those that target the PI3K/AKT pathway.

Recent evidence suggested that combinatory targeted therapies could result in enhanced treatment efficacy. For instance, MAPK and PI3K/AKT are simultaneously and synergistically activated in a *Pten*$^{+/-}$ mouse prostate model (Gumerlock et al, 1997). Our genetically modified (*Nkx Cre Pten*$^{+/-}$ *Spry2*$^{+/-}$) mouse model showed evidence of PI3K/AKT hyper-activation, without MAPK activation, in the prostate (Fig 6C) and enhanced capability to develop metastatic nodal disease by 12 months. Significantly, the PI3K inhibitor PI103 exerted a dramatic inhibitory effect on the development of nodal metastasis. Taken together, the selective activation of PI3K/AKT associated with SPRY2 loss in the context of PTEN insufficiency is important in prostate carcinogenesis: PI3K/AKT function enhances EGFR/HER2 signalling via activation of p38; PI3K/AKT promotes a proliferative and invasive phenotype *in vitro* and *in vivo*; suppression of PI3K/AKT function reverse the above *in vitro* and *in vivo* phenotype; and finally, upregulated p-AKT expression was closely associated with reduced SPRY2 expression in clinical PC. Interestingly, among our PC TMA cohorts, the majority of them have moderate PTEN expression, with around 25% of our PC cases exhibiting complete PTEN loss (histoscore = 0). The impact of SPRY2 loss in clinical PC was further confirmed. First, patients with PC showing reduced SPRY2 and enhanced HER2 expression have a shorter overall survival. Second, SPRY2 loss is closely associated with upregulated cytoplasmic HER2 expression as well as enhanced p-AKT level but not ERK activation (Supporting Information Table 1). Intriguingly, in the patient sub-group with complete PTEN loss (25%), the association between SPRY2 loss and p-AKT activation was lost, while the relationship between SPRY2 and HER2 switched from a negative to a positive association with reduced HER2 expression in tumours showing SPRY2 loss ($p < 0.01$, $r = 0.258$). These data are consistent with two further observations: (1) The prognostic value of HER2 was lost in these PTEN-negative tumours (Supporting Information Fig S3d) and (2) In SPRY2-positive tumours, HER2 was not prognostic for patient outcomes (Supporting Information Fig S3e). This finding is in keeping with our *in vitro* observation that, in the presence of complete PTEN loss, the level of EGFR appeared to be very low upon suppression of SPRY2 expression. In conclusion, complex interactions among RTKs and their downstream effectors exhibit fine regulation of the signalling networks to involve distinct signalling molecules (Fig 8), which may represent important targets for developing treatment in the context of personalized medicine.

MATERIALS AND METHODS

Cell culture and cell growth assay

Human PC cell lines, DU145 and PC3 were authenticated by LCG standards. Cells were grown in RPMI (Gibco) containing 10% serum supplement in a humidified incubator (37°C, 5% CO_2). For cell proliferation assays, WST-1 reagent (Roche Applied Science) was used in a 96-well plate as described in the manufacture's instruction. Cells were stimulated with EGF at 20 ng/ml following overnight serum starvation. Data obtained from individual cell lines maintained in serum-free condition without EGF stimulation were used as the reference. The percentage increase in cell growth was calculated from

The paper explained

PROBLEM:

Treatment for incurable or recurrent prostate cancer (PC) remains a major clinical problem worldwide and targeted therapies against receptor tyrosine kinases (RTKs) in PC have not been promising. Intracellular regulators of RTKs are increasingly implicated to have a potential role in PC, but the clinical and pre-clinical *in vivo* evidence for this are lacking.

RESULTS:

Here, for the first time, our report implicates the interaction between PTEN and SPRY2 to regulate the function of ErbB receptor by promoting receptor internalization and sustained localization at the early endosome. This is associated with enhanced PI3K/AKT signalling activities both *in vitro* and *in vivo*. Furthermore, our data suggest that ErbB-positive PC with SPRY2 loss and partial inactivation of PTEN are particularly susceptible to PI3K/AKT-targeted therapy, which can be exploited as a basis of personalized therapy for patient with PC. In addition, complete loss (or functional negligent level) of PTEN combined with impaired SPRY2 expression resulted in RTK (EGFR and HER2) degradation, thus paradoxically rendering the tumour cells insensitive to therapies targeting these receptors.

IMPACT:

Complex interactions among RTKs and their downstream effectors exhibit fine regulation of the signalling networks to involve distinct signalling molecules, which may represent important targets for developing treatment in the context of personalized medicine.

(and normalized against) the respective data from the serum- and EGF-free control for each cell clone.

shRNA and siRNA transfection

For generation of stable SPRY2 KD cell lines, we used a 19 mer sprouty2 target sequence (5′-AACACCAATGAGTACACAGAG-3′), and Nsi control sequence was obtained from Qiagen. Plasmid pTER+ were used to insert the sequence of interest, and stably expressed in DU145, PC3 and 22Rv1 cell lines. SPRY2 expression construct used for stable and transient expression was a kind gift from Graeme Guy (Institute of Molecular and Cell Biology, Singapore). LNCaP cells stably expressing SPRY2 were selected using geneticin (200 μg/ml, Gibco). For transient SPRY2 siRNA transfection, two different siRNA sequences were purchased from Dharmacon, and PTEN and p38 siRNA was obtained from cell signalling. Transfection was carried out with Amaxa Cell Line Nucleofactor Kit (Lonza). The PTEN expression construct (EGFP-PTEN) was generated by cloning PTEN cDNA (OriGene) into EcoRI/SalI-cut EGFPC2 (Clontech) vector, and the plasmid was transfected using Lipofectamine™ 2000 (Invitrogen) as described manufacture's protocol.

Invasion assay

For invasion assay, invasion transwell chambers (BD Sciences) with 8 μm pore were used as described in the manufacture's instruction. Briefly, the matrigel-coated transwells were rehydrated and 40,000 cells were seeded in triplicate. After 8 h incubation with EGF (20 ng/ml) as a chemo-attractant, the upper surface cells were removed. The 'invaded' cells at the lower surface of the membrane were fixed and stained with DAPI. In absence of EGF as chemo-attractant, we observed negligible numbers of invading cells.

Western blot analysis

Cell lines or tissue lysates were generated, and the protein concentration of whole cell lysates was determined using the Bradford method (Bio-Rad) according to the manufacturer's instructions. Samples were stored in −80°C. Loading controls including actin, tubulin and GAPDH were used.

For analysis using the Human Phospho-Kinase array (R&D), cells were serum starved, EGF (20 ng/ml) stimulated for 15 min lysed and then incubated with the array membranes according to manufacturer's instructions, following by signal development and analysis with image J.

Antibodies used for Western blotting

Antibodies against p-AKT (Ser473), p-EGFR, EGFR, p-p38, p38, p44/42, p-p44/42 (p-ERK) MAPK (Thr202/Tyr204), p-HER2, HER2, p-mTOR, PTEN, ATF2 and p-ATF2 were obtained from Cell signalling. Actin (Sigma), and GAPDH (Sigma) were used as loading controls.

Immunofluorescence

Cells were grown on glass bottom micro-plates (Mat Tek), and transfected with EEA1-EGFR plasmid for 16 h. Cells were stimulated with EGF and fixed in 4% PFA at the indicated time points for 15 min, and permeablized in 0.1% Triton for 5 min. EGFR antibody (BD Sciences) incubation was done after blocking in 1% FBS and 0.5% BSA in PBS for 1 h. Secondary antibodies were purchased from Invitrogen.

Internalization assay

EGFR internalization assays were performed after overnight serum starvation followed by EGF treatment (20 ng/ml) as described previously (Sarto et al, 2007). Internalization assays were performed in the presence of 0.6 mM of primaquine. For immunoprecipitation (IP), the internalization was performed and immunoprecipitated the biotin labelled EGFR with dynabeads instead of ELISA plates.

Immunoprecipitation (IP)

IP for EGFR and HER2 was performed following the internalization assay step using Dynabeads® Sheep anti-Mouse IgG (Invitrogen) coupled to EGFR antibody (BD Sciences) and NeutrAvidin Agarose

(Thermo Scientific), respectively. The beads were then boiled in loading buffer without reducing agent and then analysed by Western bloting.

RT-PCR

RNA was extracted from PC3 SPRY2 KD and Nsi control cell lines using RNeasy mini kit (Qiagen) as described by the manufactor. cDNA was synthesized using High Capacity cDNA Reverse Transcription Kits (Applied Biosystem) as described by the manufacturer's instruction. The relative mRNA levels were assessed by quantitative PCR (Roche Applied Science) using an SYBR Green PCR kit (Fermentas). Primers were designed using Primer3 software, and the specific sequences for EGFR and GAPDH were sense: 5′-GAGGTGGTCCTTGGGAATTT-3′, antisense: 5′-GGAATTCGCTCCACTGTGTT-3′, and sense: 5′-GGGAAGCTTG TCATCAATGG-3′, and antisense 5′-TGGACTCCACGACGTACTCA-3′, respectively. Signals were normalized to GAPDH as internal control.

Mouse work and tumour studies

Nkx 3.1-Cre (Hsieh et al, 2010) mice were crossed to those harbouring *Spry2*$^{+/-}$ (Shim et al, 2005), and *Pten*$^{+/-}$ (Lesche et al, 2002), and mice were genotyped by PCR by Transnetyx^{TM} (Andrechek et al, 2000; Lesche et al, 2002; Shim et al, 2005). Mice of a mixed background and littermates were used as control mice. The prostates and lymph nodes were placed in formalin for overnight fixation before paraffin embedding. All experiments were carried out in accordance with the Project Licence (PPL 60/3947) under Home Office Animal (Scientific Procedures) Act 1986 in the UK.

PI3K inhibitor treatment

PI103 treatment was commenced when tumours were expected to have developed in the *Spry2*$^{+/-}$ *Pten*$^{fl/+}$ mice at age of 10–11 months. PI103 was injected daily at 50 mg/kg i.p for 4 weeks. At the end of the experimental period, prostate tissues were collected and fixed in formalin or frozen in liquid nitrogen.

Immunohistochemistry

Tissue samples were formalin fixed, paraffin-embedded, and at least three samples from three different mice were analysed. For Ki67 staining, Ki67 antibody (Vector Labs) was used at 1/100 dilution, and antigen unmasking was performed in citrate buffer and water bath incubation for 50 min at 99°C. For p-AKT (ser473; Cell Signaling, 1/50 dilution) and p-ERK1/2 (Cell Signaling, 1:100 dilution), citrate buffer and microwave antigen retrieval method was used.

TUNEL assay

Cell death was detected by TUNEL assay (Calbiochem). As described by the manufacturer, briefly paraffin-embedded tissue slides were deparaffinized and rehydrated. Endogenous peroxidases were inactivated. DNA fragments were labelled with TdT Enzyme, and detected with DAB solution.

Tissue microarray analysis of human

With local ethical committee approval (MREC 01/0/36), formalin-fixed paraffin-embedded (FFPE) sections were studied. 3×0.6 mm^2 cores of PC tissue as identified by pathologists were removed from representative areas of the FFPE blocks. All samples had been taken from PC patients at the time of trans-urethral resection of the prostate (TURP), and graded by consultant pathologist. These samples were processed by IHC. Survival analysis was performed using Kaplan–Meier plot and log rank test.

Statistics

All the statistical analysis was performed using Prism 5 software including student's *t*-test and one-way ANOVA, and all graphs were generated using Microsoft Excel software. The error bars were calculated and represented in terms of mean ± SD or s.e.m.

Author contributions

MG, RP and HYL designed experiments and interpreted data; MG, RP and JF carried out *in vitro* cell experiments; MG, RP and IA carried out *in vivo* experiments on mouse models; JN assist in receptor cycling experiments; OS supported *in vivo* transgenic mouse models; JE, SMcC, KS, MS and HYL are involved in the preparation of tissue microarray and collection of clinical information for clinical samples; IA, JE, SMcC, KS and HYL carried out the data analysis; MG and HYL wrote the manuscript.

Acknowledgements

This work was funded by Cancer Research UK. We thank for the technical support from BICR core services at the biological services unit and Colin Nixon for histology service. The 'Think Pink' charity part funded the Aperio slide scanner and the Slidepath software. We are grateful to Gail Martin (University of California San Francisco) and Albert Basson (King's College London) for providing the Sprouty 2 transgenic mouse model.

Supporting Information is available at EMBO Molecular Medicine online.

The authors declare that they have no conflict of interest.

References

Andrechek ER, Hardy WR, Siegel PM, Rudnicki MA, Cardiff RD, Muller WJ (2000) Amplification of the neu/erbB-2 oncogene in a mouse model of mammary tumorigenesis. Proc Natl Acad Sci USA 97: 3444-3449

Baluk P, Fuxe J, Hashizume H, Romano T, Lashnits E, Butz S, Vestweber D, Corada M, Molendini C, Dejana E, *et al* (2007) Functionally specialized junctions between endothelial cells of lymphatic vessels. J Exp Med 204: 2349-2362

Bordoni V, Alonzi T, Zanetta L, Khouri D, Conti A, Corazzari M, Bertolini F, Antoniotti P, Pisani G, Tognoli F, *et al* (2007) Hepatocyte-conditioned medium sustains endothelial differentiation of human hematopoietic-endothelial progenitors. Hepatology 45: 1218-1228

Carracedo A, Alimonti A, Pandolfi PP (2011) PTEN level in tumor suppression: How much is too little? Cancer Res 71: 629-633

Carver BS, Chapinski C, Wongvipat J, Hieronymus H, Chen Y, Chandarlapaty S, Arora VK, Le C, Koutcher J, Scher H, *et al* (2011) Reciprocal feedback regulation of PI3K and androgen receptor signaling in PTEN-deficient prostate cancer. Cancer Cell 19: 575-586

Chandarlapaty S, Sawai A, Scaltriti M, Rodrik-Outmezguine V, Grbovic-Huezo O, Serra V, Majumder PK, Baselga J, Rosen N (2011) AKT inhibition relieves feedback suppression of receptor tyrosine kinase expression and activity. Cancer Cell 19: 1-14

Danese S, Dejana E, Fiocchi C (2007) Immune regulation by microvascular endothelial cells: directing innate and adaptive immunity, coagulation, and inflammation. J Immunol 178: 6017-6022

Dejana E, Taddei A, Randi AM (2007) Foxs and Ets in the transcriptional regulation of endothelial cell differentiation and angiogenesis. Biochim Biophys Acta 1775: 298-312

Edwin F, Singh R, Endersby R, Baker SJ, Patel TB (2006) The tumor suppressor PTEN is necessary for human Sprouty 2-mediated inhibition of cell proliferation. J Biol Chem 281: 4816-4822

Faratian D, Sims AH, Mullen P, Kay C, Um I, Langdon SP, Harrison DJ (2011) Sprouty 2 is an independent prognostic factor in breast cancer and may be useful in stratifying patients for trastuzumab therapy. PloS ONE 6: e23772

Fritzsche S, Kenzelmann M, Hoffmann MJ, Muller M, Engers R, Grone HJ, Schulz WA (2006) Concomitant down-regulation of SPRY1 and SPRY2 in prostate carcinoma. Endocr Relat Cancer 13: 839-849

Goltsov A, Faratian D, Langdon SP, Mullen P, Harrison DJ, Bown J (2012) Features of the reversible sensitivity-resistance transition in PI3K/PTEN/AKT signalling network after HER2 inhibition. Cell Signal 24: 493-504

Gumerlock PH, Chi SG, Shi XB, Voeller HJ, Jacobson JW, Gelmann EP, Devere White RW (1997) p53 abnormalities in primary prostate cancer: single-strand conformation polymorphism analysis of complementary DNA in comparison with genomic DNA. The Cooperative Prostate Network. J Natl Cancer Inst 89: 66-71

Hacohen N, Kramer S, Sutherland D, Hiromi Y, Krasnow MA (1998) sprouty encodes a novel antagonist of FGF signaling that patterns apical branching of the *Drosophila* airways. Cell 92: 253-263

Hsieh AC, Costa M, Zollo O, Davis C, Feldman ME, Testa JR, Meyuhas O, Shokat KM, Ruggero D (2010) Genetic dissection of the oncogenic mTOR pathway reveals druggable addiction to translational control via 4EBP-eIF4E. Cancer cell 17: 249-261

Kawakami Y, Kubota N, Ekuni N, Suzuki-Yamamoto T, Kimoto M, Yamashita H, Tsuji H, Yoshimoto T, Jisaka M, Tanaka J, *et al* (2009) Tumor-suppressive lipoxygenases inhibit the expression of c-myc mRNA coding region determinant-binding protein/insulin-like growth factor II mRNA-binding protein 1 in human prostate carcinoma PC-3 cells. Biosci Biotechnol Biochem 73: 1811-1817

Kim MJ, Bhatia-Gaur R, Banach-Petrosky WA, Desai N, Wang Y, Hayward SW, Cunha GR, Cardiff RD, Shen MM, Abate-Shen C (2002a) Nkx3.1 mutant mice recapitulate early stages of prostate carcinogenesis. Cancer Res 62: 2999-3004

Kim MJ, Cardiff RD, Desai N, Banach-Petrosky WA, Parsons R, Shen MM, Abate-Shen C (2002b) Cooperativity of Nkx3.1 and Pten loss of function in a mouse model of prostate carcinogenesis. Proc Natl Acad Sci USA 99: 2884-2889

Kim HJ, Taylor LJ, Bar-Sagi D (2007) Spatial regulation of EGFR signaling by Sprouty2. Curr Biol 17: 455-461

Kim J, Eltoum IE, Roh M, Wang J, Abdulkadir SA (2009) Interactions between cells with distinct mutations in c-MYC and Pten in prostate cancer. PLoS Genet 5: e1000542

Lesche R, Groszer M, Gao J, Wang Y, Messing A, Sun H, Liu X, Wu H (2002) Cre/loxP-mediated inactivation of the murine Pten tumor suppressor gene. Genesis 32: 148-149

Mckie AB, Douglas DA, Olijslagers S, Graham J, Omar MM, Heer R, Gnanapragasam VJ, Robson CN, Leung HY (2005) Epigenetic inactivation of the human sprouty2 (hSPRY2) homologue in prostate cancer. Oncogene 24: 2166-2174

Mellinghoff IK, Vivanco I, Kwon A, Tran C, Wongvipat J, Sawyers CL (2004) HER2/neu kinase-dependent modulation of androgen receptor function through effects on DNA binding and stability. Cancer cell 6: 517-527

Nishimura M, Shin MS, Singhirunnusorn P, Suzuki S, Kawanishi M, Koizumi K, Saiki I, Sakurai H (2009) TAK1-mediated serine/threonine phosphorylation of epidermal growth factor receptor via p38/extracellular signal-regulated kinase: NF-{kappa}B-independent survival pathways in tumor necrosis factor alpha signaling. Mol Cell Biol 29: 5529-5539

Potente M, Ghaeni L, Baldessari D, Mostoslavsky R, Rossig L, Dequiedt F, Haendeler J, Mione M, Dejana E, Alt FW, *et al* (2007) SIRT1 controls endothelial angiogenic functions during vascular growth. Genes Dev 21: 2644-2658

Rubin C, Litvak V, Medvedovsky H, Zwang Y, Lev S, Yarden Y (2003) Sprouty fine-tunes EGF signaling through interlinked positive and negative feedback loops. Curr Biol 13: 297-307

Sarto P, Balducci E, Balconi G, Fiordaliso F, Merlo L, Tuzzato G, Pappagallo GL, Frigato N, Zanocco A, Forestieri C, *et al* (2007) Effects of exercise training on endothelial progenitor cells in patients with chronic heart failure. J Card Fail 13: 701-708

Shen MM, Abate-Shen C (2010) Molecular genetics of prostate cancer: new prospects for old challenges. Genes Dev 24: 1967-2000

Shim K, Minowada G, Coling DE, Martin GR (2005) Sprouty2, a mouse deafness gene, regulates cell fate decisions in the auditory sensory epithelium by antagonizing FGF signaling. Dev Cell 8: 553-564

Slack A, Chen Z, Tonelli R, Pule M, Hunt L, Pession A, Shohet JM (2005) The p53 regulatory gene MDM2 is a direct transcriptional target of MYCN in neuroblastoma. Proc Natl Acad Sci USA 102: 731-736

Song MS, Carracedo A, Salmena L, Song SJ, Egia A, Malumbres M, Pandolfi PP (2011) Nuclear PTEN regulates the APC-CDH1 tumor-suppressive complex in a phosphatase-independent manner. Cell 144: 187-199

Taylor BS, Schultz N, Hieronymus H, Gopalan A, Xiao Y, Carver BS, Arora VK, Kaushik P, Cerami E, Reva B, *et al* (2010) Integrative genomic profiling of human prostate cancer. Cancer cell 18: 11-22

Traish AM, Morgentaler A (2009) Epidermal growth factor receptor expression escapes androgen regulation in prostate cancer: a potential molecular switch for tumour growth. Br J Cancer 101: 1949-1956

Trotman LC, Niki M, Dotan ZA, Koutcher JA, Di Cristofano A, Xiao A, Khoo AS, Roy-Burman P, Greenberg NM, Van Dyke T, *et al* (2003) Pten dose dictates cancer progression in the prostate. PLoS Biol 1: E59

Voeller HJ, Augustus M, Madike V, Bova GS, Carter KC, Gelmann EP (1997) Coding region of NKX3.1, a prostate-specific homeobox gene on 8p21, is not mutated in human prostate cancers. Cancer Res 57: 4455-4459

Weber C, Fraemohs L, Dejana E (2007) The role of junctional adhesion molecules in vascular inflammation. Nat Rev Immunol 7: 467-477

Woodfin A, Reichel CA, Khandoga A, Corada M, Voisin MB, Scheiermann C, Haskard DO, Dejana E, Krombach F, Nourshargh S (2007) JAM-A mediates neutrophil transmigration in a stimulus-specific manner *in vivo*: evidence for sequential roles for JAM-A and PECAM-1 in neutrophil transmigration. Blood 110: 1848-1856

Zhang H, Hu G, Wang H, Sciavolino P, Iler N, Shen MM, Abate-Shen C (1997) Heterodimerization of Msx and Dlx homeoproteins results in functional antagonism. Mol Cell Biol 17: 2920-2932

Zwang Y, Yarden Y (2006) p38 MAP kinase mediates stress-induced internalization of EGFR: implications for cancer chemotherapy. EMBO J 25: 4195-4206

